Review

Multi-Modality Cardiovascular Imaging Assessment in Fabry Disease

Ashwin Roy [1,2,*], Mohamed Mansour [2], David Oxborough [3], Tarekegn Geberhiwot [2,4] and Richard Steeds [1,2]

1   Institute of Cardiovascular Sciences, University of Birmingham, Edgbaston, Birmingham B15 2TT, UK; rick.steeds@uhb.nhs.uk
2   University Hospitals Birmingham NHS Foundation Trust, Centre for Rare Diseases, Queen Elizabeth Hospital, Mindelsohn Way, Birmingham B15 2GW, UK; mohamed.mansour@uhb.nhs.uk (M.M.); tarekegn.geberhiwot@uhb.nhs.uk (T.G.)
3   School of Sport and Exercise Sciences, Liverpool John Moores University, Tom Reily Building, Byrom Street, Liverpool L3 3AF, UK; d.l.oxborough@ljmu.ac.uk
4   Institute of Metabolism and Systems Research, University of Birmingham, Edgbaston, Birmingham B15 2TT, UK
*   Correspondence: ashwinroy@nhs.net

Abstract: Fabry disease (FD) is a rare X-linked lysosomal storage disorder manifesting as progressive multi-organ accumulation of sphingolipids due to deficiency in the enzyme α-Galactosidase A. Sphingolipid accumulation can take place in all cardiac cell types which manifests as left ventricular hypertrophy, microvascular ischaemia, conduction abnormalities, arrhythmia, heart failure, and valvular disease. The use of advanced cardiovascular imaging techniques have enabled clinicians to stage and prognosticate the disease and guide therapy. Transthoracic echocardiography (TTE) and cardiac magnetic resonance imaging (CMR) in conjunction are the hallmark imaging modalities to allow for this assessment. Traditionally, the assessment of cardiac involvement in FD was based on the assessment of maximal wall thickness (MWT) and the development of left ventricular hypertrophy (LVH). It is now understood that sphingolipid accumulation takes place before the development of LVH. Advances in techniques within TTE and CMR, particularly that of strain assessment and T1/T2 mapping, have meant that Fabry cardiomyopathy (FCM) can be diagnosed earlier in the disease process. This potentially provides a window for initiation of enzyme replacement therapy (ERT) at a stage where it is likely to have the most beneficial effect in reducing the high mortality associated with FCM. This review outlines the advances in multimodality imaging in staging and prognosticating FCM, as well as the applications of cardiac imaging in assessing symptoms and complications of FCM.

1. Introduction

Fabry disease (FD) is an X-linked lysosomal storage disorder, which manifests as a deficiency in the enzyme α-Galactosidase A [1]. This leads to progressive and multi-organ accumulation of sphingolipids, particularly globotriasylceramide (Gb3) and lyso-globotriasylceramide (lyso-Gb3) [2]. Over time, this results in end-organ damage with predominant cardiac, renal, and cerebrovascular manifestations that cause significant morbidity and premature mortality [3]. Enzyme replacement therapy (ERT) and oral chaperone therapy (OCT) may stabilise renal function and cardiomyopathy if initiated early in the disease process. Sphingolipid accumulation takes place in all cardiac cell types, leading to left ventricular hypertrophy (LVH), microvascular ischaemia, conduction abnormalities, congestive cardiac failure, and valvular disease. Prevalence is estimated to be between 1:40,000 and 1:117,000 live births. Although Fabry disease is rare, it serves as a

paradigm for the application of modern cardiovascular imaging techniques in diagnosis, guiding therapy and determining prognosis. The aim of this article is to outline the advantages of state-of-the-art imaging in the staging, management, and prognosticating of patients with FD.

2. Diagnosis: Maximal Wall Thickness and LV Hypertrophy

2.1. Transthoracic Echocardiography

Transthoracic echocardiography (TTE) is a readily available and accessible imaging modality that is widely used for screening, assessment, and monitoring of cardiac involvement in FD by determining systolic and diastolic function, left ventricular (LV) mass, LV wall thickness (LVWT), presence of left ventricular outflow tract obstruction (LVOTO), and the presence of valvular heart disease [4]. In those with confirmed 'classical' variant FD (in whom leucocyte enzyme activity is less than 5%), Fabry-specific therapy is considered at the point of diagnosis of the phenotype [5]. In those with 'later onset' variants, TTE imaging triggers the initiation of ERT or OCT in patients with a maximum wall thickness (MWT) >12 mm in males and >11 mm in females [6], or an increase in LV mass above the normal range for age and sex (see Figure 1). American and European guidelines on chamber quantification specify that measurements of wall thickness and mass should be performed using 2D echocardiography [7]. Specifically, linear measurements of wall thickness should be obtained by 2D echocardiographic images to avoid oblique sections of the LV (see Figure 1). For LV mass, 2D area-length or truncated ellipsoid techniques are recommended where LV mass is to be measured in an individual over time, especially in cases when LV geometry may be abnormal, as in FD. Unfortunately, recent data have emphasized how highly variable these 2D techniques are, even when used by internationally recognized experts. In a study analysing the measurements of 70 experienced readers from across the world, using 2D images that were in the majority graded as good quality, intramodality inter-reader percentage variability was large (range −59% to 117% (SD 20%)) [8]. Furthermore, the variability of measuring LV mass using 2D methods is also high, both significantly over-estimating LV mass and with wide inter-observer variability, such that measures can differ to the order of 9–10 g [9]. The advent of 3D echocardiography has made this the technique of choice, mainly because it is the only echocardiographic technique that directly measures myocardial volume. Although data consistently support the use of 3D compared to 2D techniques both in terms of accuracy and reproducibility, variability remains a problem, with 95% limits of agreement in measurement of LV mass still as high as 28%, and inter (7%) and intra-observer (8%) variability much greater than expected [10]. With technical improvements in spatial and temporal resolution that can achieve whole heart, single beat high resolution 3D datasets, this variability is falling to the extent that with semi-automated analysis, variability of repeated measures is below 5% [11]. With artificial intelligence (AI) increasingly used for analysis of data, and technical developments in cardiac ultrasound, it is likely that accuracy will compete with cardiovascular magnetic resonance (CMR) imaging.

2.2. Cardiac MRI

Cardiac MRI is considered the gold standard non-invasive tool for measuring MWT and LV mass based on multiple studies, relying on the acquisition of serial short-axis balanced steady-state free precession (SSFP) images along perpendicular long axis images of the ventricle. In FD, the clinical impact of the use of CMR in preference to 2D echocardiography has been emphasised in a retrospective study of 78 patients in whom eligibility for disease-specific therapy changed in more than one out of four patients (26%) [12]. TTE consistently over-estimated both MWT and LV mass, suggesting that FD patients frequently are liable to over-estimated MWT and LV mass. These results were replicated in another study of 32 patients with FD (47% male), in whom the highest variability in MWT was the LV inferolateral wall and with consistent over-estimation of LV mass using 2D echocardiography [13].
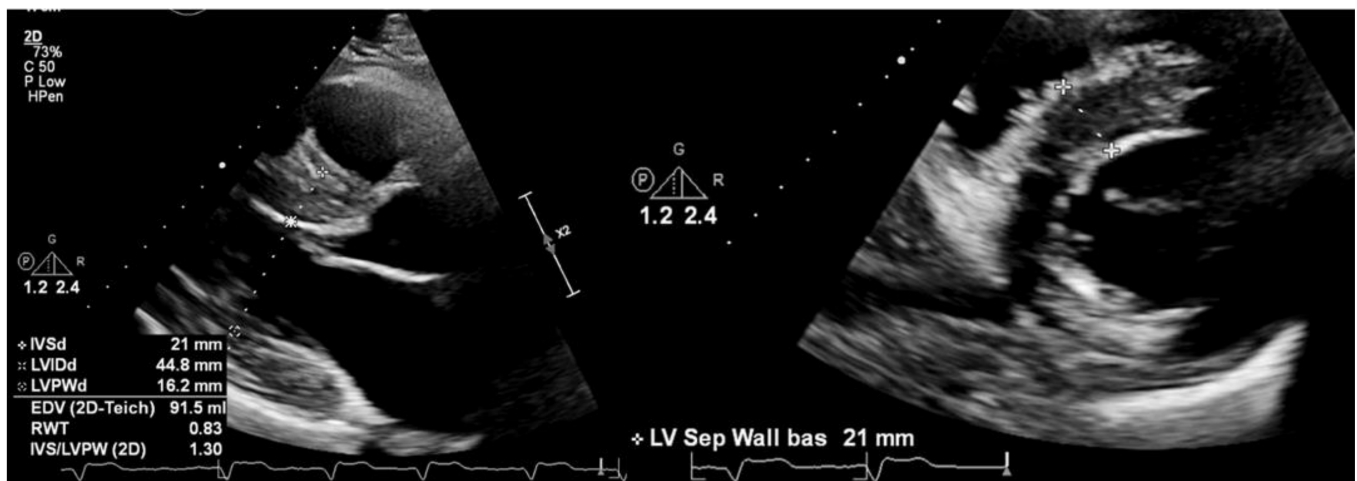
Figure 1. (**Left**) Parasternal long axis 2D TTE demonstrating linear measurements of IVS, LVID and LVPW demonstrating severe LVH; (**Right**) Parasternal short axis 2D TTE demonstrating severe LVH with MWT of 21 mm. Both images are taken from an adult male with advanced cardiomyopathy related to FD.

Most data for wall thickness and mass on CMR have been produced using semi-automatic software that analyse short axis images on a per slice basis, deriving LV mass and volume by applying the Simpsons' stack of discs' method (see Figure 2). Two issues that continue to affect inter-study repeatability are the selection of the basal slice and consistency in the method used for contouring selected, in terms of detailed contouring [14] as opposed to smooth contouring [15]. Both of these factors can make a big difference to serial assessment in a given individual, with re-classification of 20% of patients with hypertrophy to normal LV mass if using smoothed contours, the latter technique tending to under-estimate measurements particularly in those patients with papillary muscle hypertrophy as is typical of FD [16]. As in echocardiography, the limitations of measurements made by expert readers of MWT have been highlighted in comparison to those made using AI. Figure 3 demonstrates this by indicating the high degree of variability between manual contouring by experts and semi-automated AI quantification of MWT. In a large multicentre study of 60 HCM patients scanned twice, MWT measured by a machine learning algorithm was more precise and reproducible on test–retest than those of 11 human experts. Adoption of machine learning tools may have significant implications for the selection of FD patients to start therapy or to refer for device therapy, with expert test–retest differences ranging from 1.1 to 3.7 mm difference, compared to only 0.7 mm for AI [17].
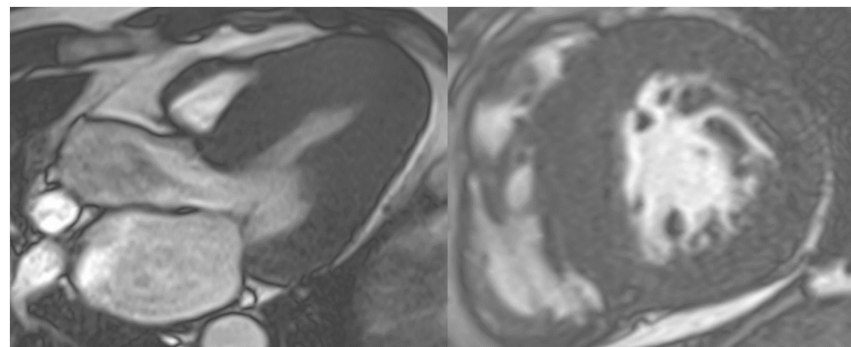

Figure 2. CMR cine imaging in a patient with Fabry cardiomyopathy; (**Left**) Apical 3-chamber view demonstrating concentric LVH with basal inferolateral wall-thinning; (**Right**) CMR short axis image demonstrating severe concentric LVH.
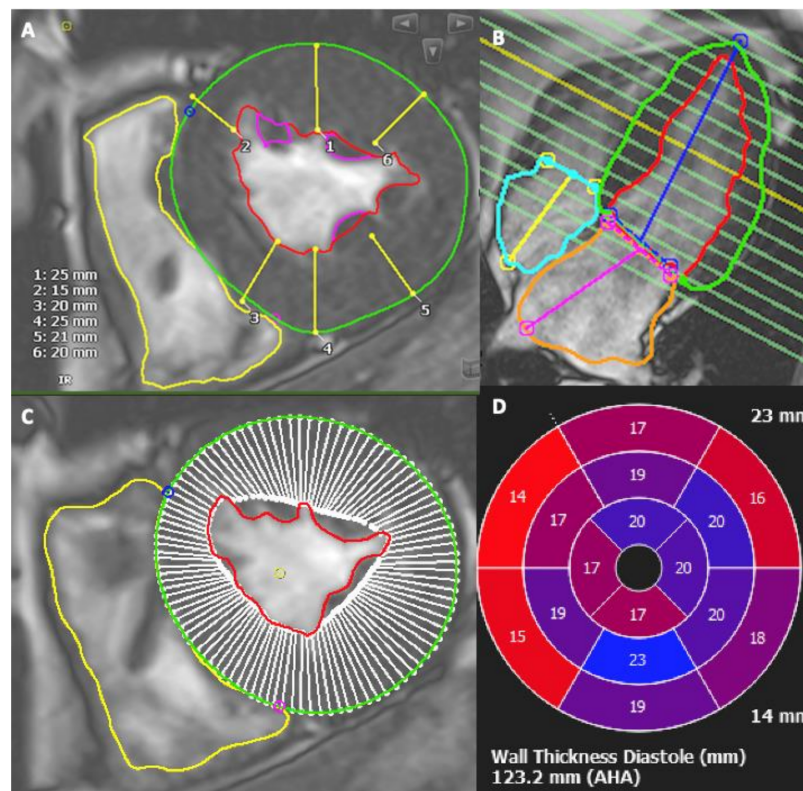
Figure 3. CMR analysis of wall thickness using manual contouring versus AI. (**A**): Manual contouring and corresponding quantification of MWT using a 3D short-axis stack image of the mid-wall of the LV. (**B**): Corresponding 4-chamber view demonstrating the mid-wall slice through the LV where the manual/AI contouring is completed. (**C**): Semi-automated AI-generated quantification of wall thickness derived from 3D short axis imaging demonstrating end-diastolic MWT. (**D**): Corresponding map of AI-generated MWT measurements (millimetres) from base-apex of the LV. Images contoured and semi-automated AI conducted using cvi42 version 5.11.2 (Circle Cardiovascular Imaging, Calgary, AB, Canada).

Summary points:

- LV maximal wall thickness and LVH are important triggers to treatment in FD;
- Measurement of MWT is highly variable in expert hands-on 2D echocardiography and CMR;
- Further work should be addressed at validating AI-based analysis of 3D echocardiography and CMR stacks in this population with the aim for this to eventually become the gold standard.

3. Diagnosis: Tissue Characterization in Early Disease

Although diagnosis of cardiac phenotype in FD has hitherto been based primarily on measurement of MWT and development of LVH, it is understood that sphingolipid deposition precedes the development of hypertrophy and is a continuous process that results in insidious progression of organ involvement over time. In most men with a classical phenotype, LVH develops in their 30 s, and in most women approximately 10 years later [18], then continues to rise inexorably regardless of treatment with ERT [19]. Data consistently suggest that ERT, and perhaps OCT, have the most significant effect on stabilizing cardiac disease if given early enough [20]. A critical development in advanced cardiovascular imaging techniques is the detection of cardiac involvement before the onset of LVH, an aim that is particularly suited to innovative imaging tools both in echocardiography and CMR.

3.1. Transthoracic Echocardiography

Reduction in age-adjusted tissue Doppler (TDI) systolic (s') velocity and early myocardial relaxation velocity (e') is a consistent early finding in FD cardiomyopathy (see Figure 4). Case–cohort studies have demonstrated a reduction in both s' and e' in gene-positive, phenotype negative patients compared to normal controls. This reduction was intermediate in size compared to that found in gene-positive patients with LVH. This has been demonstrated not only in sarcomeric HCM mutations [21], but also in a study of 20 patients with FD (10 with LVH, 10 without) and 10 age- and sex-matched controls, a reduction that takes place regardless of gender and mutation. Subsequent histological examination of endomyocardial biopsies demonstrated that reductions in TDI velocities were proportionate to the accumulation of sphingolipid in the gene+/LVH+ group and the gene+/LVH- group compared to controls. Furthermore, the observed reduced tissue velocities in the gene+/LVH- group correlated with higher LV end-diastolic filling pressures during cardiac catheterization [22]. Moreover, introduction of therapy based on reduced TDI velocities before development of LVH may be advantageous. In a study of 76 patients, the finding of reduced s' and e' prior to onset of LVH was not only replicated but the severity of reduction was also found to be inversely proportional to the risk of developing LVH. When comparing LVH- patients, 80% went on to develop abnormal TDI without ERT compared with 33% on ERT [23]. The limitation of TDI in clinical practice is that, although case–control studies consistently differentiate gene+/LVH+ from gene+/LVH- and controls, the absolute difference between the groups is small. In particular, there is considerable overlap between the values for gene+/LVH- cases and controls, meaning that defining those with an early phenotype on which to make a solid judgement about introducing treatment is difficult.
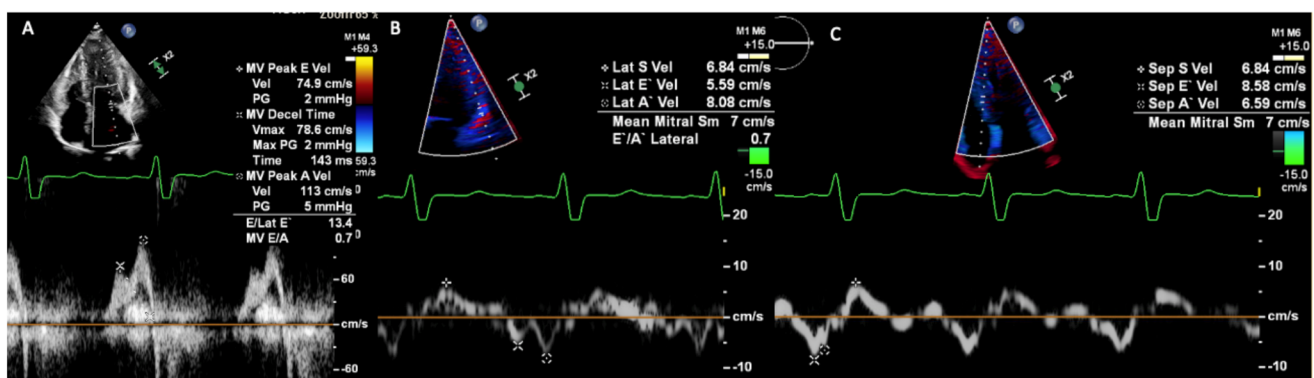

Figure 4. Pulsed-wave Doppler and TDI TTE in a patient with Fabry cardiomyopathy. (**A**): Pulsed-wave Doppler through the mitral valve leaflets showing E/A 0.7 and deceleration time 143 ms with LA dilatation; (**B**): Lateral TDI showing reduced lateral s' and e' velocities; (**C**): Septal TDI showing reduced septal s' and e' velocities.

Both Doppler-derived and 2D speckle tracking measurements of strain and strain rate are further useful developments for early detection of subclinical regional and longitudinal dysfunction in FD (see Figure 5) [24]. Impaired regional and longitudinal global longitudinal strain (GLS) has been used to quantify response to ERT [25]. In a prospective study of 16 patients with FD, longitudinal and radial strain and strain rates were significantly impaired compared to normal controls but improved over a 12 month period of treatment with ERT [24]. In an extended study of 32 FD patients over 3 years, there was evidence of benefit of early ERT based on functional improvement in 2D speckle tracking according to the presence or absence of fibrosis—in those with fibrosis documented on late enhancement imaging, both radial and longitudinal peak systolic strain rate continued to decline despite treatment, but improved in those without fibrosis [26]. These data provided some of the first evidence to suggest ERT was no longer effective when introduced later in the course of FD cardiomyopathy.
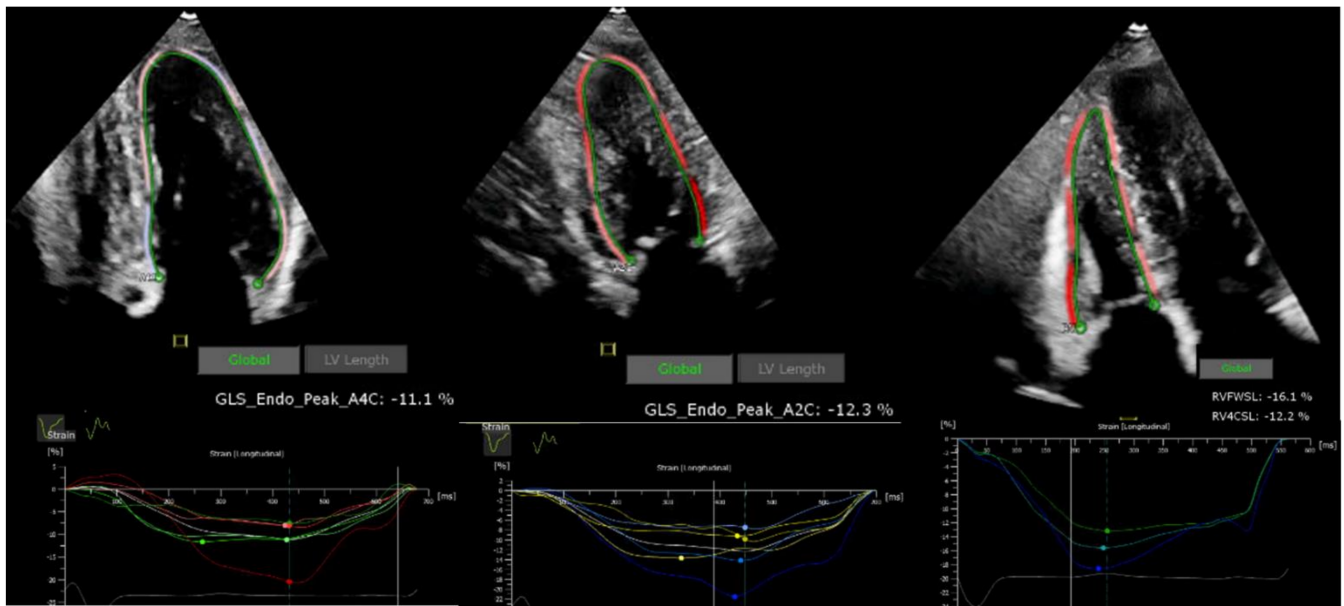
Figure 5. Strain TTE in a patient with Fabry Cardiomyopathy. **Left:** GLS assessment of the LV from the apical 4-chamber view demonstrating reduced GLS (−11.1%); **Middle:** GLS assessment of the LV from the apical 2-chamber view demonstrating reduced GLS (−12.3%); **Right:** GLS assessment of the RV from the Apical 4-chamber view demonstrating reduced GLS (free wall strain −16.1% and longitudinal strain −12.2%).

Novel technologies are emerging in identifying myocardial fibrosis in both ischaemic and non-ischaemic cardiomyopathies [27], including the use of contrast-enhanced 3D TTE, speckle tracking 3D TTE, pulse cancellation ultrasound technique, and radiomic-based analysis. Their application has not been tested in FD specifically but provides an area of future work to identify fibrosis and scar associated with FCM which enables clinicians to stage and prognosticate with both TTE and CMR.

3.2. Cardiac MRI

CMR is also able to accurately assess for early impairment of GLS similar to echocardiography (see Figure 6). However, a major advantage in performing CMR in FD patients over echocardiography has been the development of T1 mapping as an imaging biomarker of sphingolipid storage (see Figure 7). T1 mapping allows both visualization and quantification of the intracellular storage of sphingolipid, which substantially lowers T1 values below those found in other causes of LVH [28]. T1 lowering can be patchy but, unlike late enhancement imaging, is easily measured and does not require reference to 'normal' myocardium [29]. Low T1 is found in about half of FD patients before onset of LVH and appears to track both reduction in TDI and deterioration in strain values on echocardiography [30]. This may explain why a reduction in exercise capacity has been found on cardiopulmonary exercise testing in FD patients with low T1 but no other features of disease, compared to age and sex-matched controls [31]. In later stages of FD cardiomyopathy when fibrosis develops within the myocardium, typically in the basal inferolateral wall, T1 relaxation times may increase or "pseudonormalise" (see Figure 7) [32]. T1 lowering is progressive up until this 'pseudonormalisation'. Native non-contrast T1 may lengthen with interstitial expansion due to a number of processes including the development of myocardial fibrosis and inflammation, likely due to increased free fluid associated with this state [33]. T1 lowering is greater in males than females and, as with LVH-progression, the decline in values continues despite ERT [19]. Furthermore, as perhaps might be expected in an X-linked disease, T1 mapping has confirmed that there is sex-dimorphism in the development of FD cardiomyopathy, with men following a path from T1 lowering to LVH before

the development late gadolinium enhancement (LGE), whereas in women, T1 lowering can be associated with (LGE) before the development of LVH.
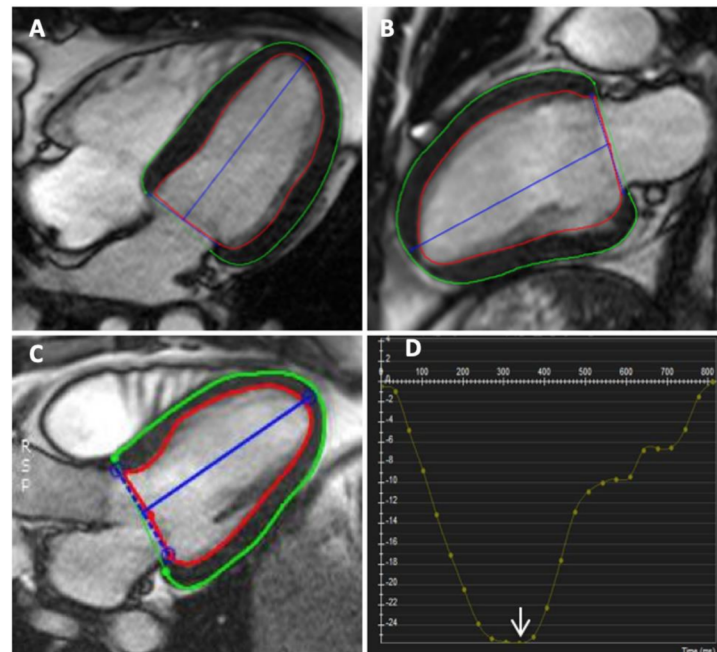

Figure 6. Long axis CMR assessment of 2D-strain using feature tracking by manually contouring endocardial and epicardial borders in end-diastole. (**A**): apical 4-chamber view, (**B**): apical 2-chamber view, (**C**): apical 3-chamber view, (**D**): myocardial strain curve with normal peak GLS measured (−26%).
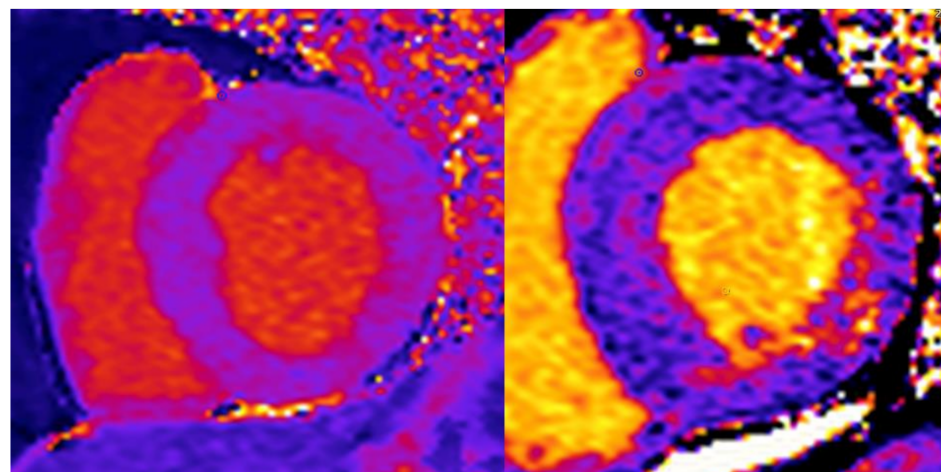

Figure 7. CMR T1 mapping at 2 disease stages in patients with FD. (**Left**) T1 map with reduced relaxation times representing early sphingolipid accumulation in a patient with Fabry and early cardiomyopathy; (**Right**) T1 map with "pseudonormalisation" of T1 representing fibrosis within the myocardium in a patient with advanced Fabry cardiomyopathy.

Low T1, however, is not always the earliest evidence of FD cardiomyopathy. In some patients, other changes can precede T1 lowering, including 12-lead electrocardiographic abnormalities, fall in global longitudinal strain (on echocardiography and CMR), diastolic dysfunction, and, less commonly, elevated biomarkers such as high-sensitive troponin [34]. T1 is an early imaging marker of cardiac involvement and, while useful as a diagnostic marker, it is not yet widely accepted as a trigger for introduction of therapy [35]. The presence of LGE, on the other hand, is an accepted trigger for therapy, despite the fact that this likely reflects a more advanced stage of disease beyond LVH [36]. The presence of LGE

in the inferolateral mid-wall is an important indicator for the diagnosis of FD, with close correlation to macroscopic fibrosis and microscopic evidence of collagen deposition in the absence of sphingolipid [37].

Summary points:

- Impairment of TDI velocity, Doppler and speckle tracking strain and strain rate are early signs of the functional impact of sphingolipid storage on the heart;
- T1 lowering is a sensitive sign of FD cardiomyopathy that precedes LVH and late gadolinium enhancement but is not yet an accepted trigger for therapy;
- Late gadolinium enhancement is an accepted trigger for initiation of therapy but there remain questions regarding efficacy once identified.

4. Diagnosis: Tissue Characterization in Later Disease

Tissue characterization on CMR has led to the concept of a staged progression of disease, through accumulation of sphingolipid to a hypertrophic phase, ultimately resulting in fibrosis and inflammation. In the final phase of fibrosis, elevated T2 values have been found in regions of fibrosis identified on LGE, that corresponded closely to elevation in high sensitivity troponin release [38]. T2 mapping, like T1 mapping, provides both a visual and quantitative assessment of intracellular and/or extracellular water, and is able to detect focal and diffuse myocardial oedema (see Figures 8 and 9). The interesting feature in FD is that T2 signal is high in areas of LGE, consistent with oedema, raising the possibility of inflammation as a final pathway in the progression of cardiomyopathy. This elevation in T1 was not found in other diseases causing LVH, such as pressure overload (aortic stenosis), extracellular expansion (amyloid) or cellular hypertrophy and disarray (sarcomeric HCM).

Figure 8. (**Left**) CMR T2 map with increased relaxation times representing oedema and inflammation within the myocardium in a patient with advanced Fabry cardiomyopathy; (**Right**) CMR LGE images with areas of LGE in the inferior and inferolateral walls of the myocardium which correspond with areas of high T2.
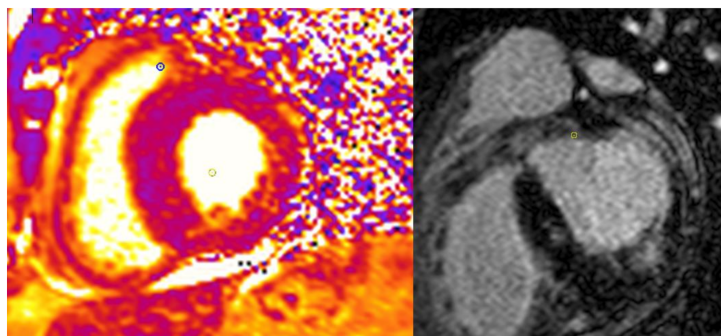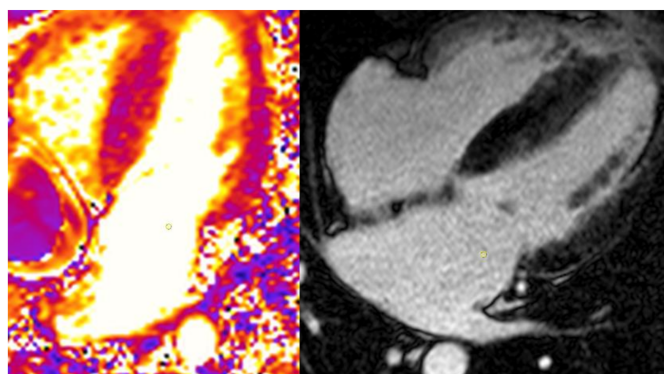

Figure 9. (**Left**) CMR T2 map with increased relaxation times representing oedema and inflammation within the myocardium in a patient with advanced Fabry cardiomyopathy; (**Right**) CMR LGE images with areas of LGE corresponding with areas of increased T2.

These CMR data build on data from other forms of advanced cardiovascular imaging, specifically 18F-FDG-positron emission tomography, that myocardial inflammation may in fact even precede development of LGE and, therefore, could be a more sustained process [39]. This was supported by data in heterozygous women with FD but no LVH, in whom focal myocardial uptake of 18F-FDG was found on PET scanning which correlated with reduction in GLS [40]. This study, therefore, linked early inflammation in FD cardiomyopathy with functional decline, before the hypertrophic phase, a finding consistent with elevation of plasma inflammatory and cardiac remodelling biomarkers [41]. The importance of these data from CMR and FDG PET are that they suggest potential alternative avenues of therapy in FD that go beyond replacement or reactivation of α-GAL enzyme.

Summary points:

- Staging disease requires a combination of echocardiography and CMR data to define a pre-hypertrophy stage when both structural and functional abnormalities can be subtle;
- Following hypertrophy, there is increasing recognition from biomarker and imaging studies that inflammation plays a role in progression to fibrosis and scar, that may coincide with altered perfusion detectable on CMR and nuclear medicine techniques.

5. Prognosis

Cardiovascular disease is now the most common cause of death in FD patients, and one of the developing roles for advanced cardiovascular imaging is in predicting prognosis. One of the major drivers for outcome in FD cardiomyopathy is the presence and severity of LVH on echocardiography or CMR, and the presence of LGE [42]. Although LVH, increased MWT and LGE may be triggers for starting treatment, there is a paucity of data however, on the incremental value of these and other functional parameters on imaging in relation to outcome.

5.1. Transthoracic Echocardiography

In a retrospective analysis of data from the Fabry Outcome Survey (FOS), the risks of cardiovascular and renal events in patients with FD established on ERT were assessed based on TTE measures. Comparisons were made between patients who were LVH+ and had impaired renal function and those who were LVH- with normal renal function at initiation of ERT. Cardiovascular events were defined as myocardial infarction, heart failure, arrhythmia, conduction abnormalities, and need for cardiac surgery. It is not surprising that cardiovascular and renal events were more common in the LVH+ and impaired renal function cohort, who were 57% more likely to have a cardiovascular end-point [43].

The ability of advanced echocardiography to define future risk in FD was replicated in a retrospective study of 96 adults with FD and normal LVEF, that assessed the ability of standard echocardiographic parameters, as well as LV GLS, myocardial mechano-energetic efficiency, and strain-based myocardial work efficiency to predict major adverse cardiac events (atrial fibrillation, ventricular tachycardia, heart failure, and death). GLS is assessed by 2D speckle tracking echocardiography and has emerged as a technique to assess early impairment in LV function. Myocardial mechano-energetics efficiency by definition is the ratio of work delivered by the myocardium versus the amount of total energy produced per heartbeat and is assessed on ultrasound. In total, 14 events occurred over a median follow-up of 63 months, and after multivariate analysis, GLS, and myocardial work indices were independently associated with a poor outcome, although myocardial mechano-energetic efficiency was not predictive [44]. Of note, both LVM and diastolic dysfunction provided additional prognostic value in detecting patients at risk of major adverse cardiac events (Cox regression analysis) which supports previous work demonstrating this in FD [42,45].

5.2. Cardiac MRI

There are limited data on the ability of CMR parameters to define long-term cardiovascular risk in FD. In a longitudinal study of 73 adults with FD over 4.8 +/− 2.4 years, serial

CMR was performed to investigate the potential for fibrosis detected using LGE to predict risk of malignant ventricular arrhythmia (incorporating non-sustained and sustained ventricular tachycardia and sudden cardiac death). In those without LGE, there were no reports of ventricular arrhythmia on Holter monitoring compared with 13 episodes of ventricular arrhythmia in those with LGE, of whom 5 experienced sudden cardiac death [46]. This finding is consistent with the established prognostic value of LGE in identifying ventricular arrhythmia risk in coronary artery disease [47] and other cardiomyopathies [48].

Imaging studies investigating prognostication in FD have tended to be small, single-centre reports and further work is needed to clarify 'what to expect' from the future in each FD patient, a process which is essential for decision-making in therapy, particularly in relation to selection of the patient for device implantation. It has long been recognized in FD that direct genotype–phenotype correlation is lacking, and the development of the phenotype is altered by a multitude of factors other than enzyme activity.

Summary points:

- Standard imaging parameters of MWT, LVH and diastolic function are predictive of cardiovascular outcome in FD;
- Advanced parameters, including GLS and MW, may independently predict risk of MACE in FD, consistent with data from other non-ischaemic cardiomyopathies but further work is required;
- Data on prognosis in FD based on CMR are limited but presence of LGE is associated with risk of malignant ventricular arrhythmia.

6. Managing Complications

6.1. Chest Pain

A series of advanced cardiovascular imaging studies have identified a complex combination of factors that lead to the common tendency for FD patients to suffer from angina. Intracellular myocyte sphingolipid deposition is only one element in the pathogenesis of cardiomyopathy, and chest pain is one symptom that is driven by a host of interacting modifiers. Myocardial hypoperfusion is an early characteristic of FD cardiomyopathy that is present in the absence of epicardial coronary stenosis, with a global reduction in coronary flow identified before onset of LVH demonstrated both using PET [49] and CMR [38]. Once LVH develops, there is the additional factor of supply–demand mismatch. This mismatch, however, may not only be due to the difference in oxygen delivery to the endocardium in a hypertrophied Fabry heart, but may also be related to altered cardiac autonomic tone in FD, identified using iodine 123 meta-iodobenzylguandidine (MIBG) [50]. Microvascular dysfunction is common due to Gb3 and lyso-Gb3 storage in the endothelium and smooth muscle cells of the microvasculature, which causes perfusion deficit on single photon emission computed tomography with 99mTC sestamibi [51]. The complexity of myocardial perfusion abnormalities is further heightened by the understanding that cholesterol profiles in FD are altered. With prolonged life expectancy due to reduction in renal-related deaths, patients are now also exposed to the environmental disease processes prevalent in the Western world that lead to accelerated atherosclerosis. Given the potential presence of perfusion abnormalities even in the absence of significant epicardial stenosis, CT coronary angiography provides an effective non-invasive modality for the identification of atherosclerosis [52].

6.2. Breathlessness

Respiratory symptoms are frequently observed in FD, including breathlessness, wheeze, and cough [53]. These may reflect both pulmonary and cardiac manifestations of FD. Lung disease associated with FD is likely due to sphingolipid deposition in bronchial cells and smooth-muscle hyperplasia with resultant bronchial constriction and airflow obstruction [54]. Biopsy studies have demonstrated smooth-muscle hyperplasia, as well as peribronchiolar fibrosis [55,56]. In a study of 17 patients with FD, cardiopulmonary involvement was assessed using exercise stress, spirometry, high-resolution computed

tomography (HRCT), and CMR. Self-reported pulmonary-related symptoms correlated with a lower EF and longer QRS duration on ECG, suggesting an overlap with cardiac manifestations relating to FD causing respiratory symptoms [57]. Left ventricular outflow tract obstruction (LVOTO) may cause breathlessness, and obstruction is seen in around two-thirds of patients with HCM [58], although incidence is low in FD [59]. In a recent case series on 14 symptomatic adults with Fabry disease, 6 patients developed dynamic LVOTO on exercise stress echocardiography that was due to a combination of systolic anterior motion of the mitral valve, in conjunction with relative reduction in LV cavity size. Dynamic stress echocardiography should, therefore, be considered for investigation of the breathless patients with Fabry disease, to confirm normal systolic response to exercise, assess for change in E/e' as a reflection of LV end-diastolic pressure, and exclude LVOTO [60].

6.3. Arrhythmia

Arrhythmia is a frequent manifestation in FD, both atrial and ventricular [61]. This is likely due to local myocardial inflammation altering the electrochemical properties of cardiomyocytes and other cell tissue [62]. The presence of left atrial (LA) dilation has been associated with new onset atrial fibrillation (AF) in the general population [63]. Impairment of LA function in the general population may also be a predictor of development of AF and may have a role in risk stratification of stroke in patients with AF [64]. LA reservoir function (expansion during ventricular systole) can be impaired in adults with FD [65] and in a retrospective cohort study of adults with FD, LA function was assessed using speckle-tracking echocardiography and compared to healthy controls. Significantly higher baseline LA dimensions were found in the FD cohort with greater phasic LA volumes and lower LA strain and strain rates. Compared with FD patients on no therapy, significant improvements in LA reservoir function, as well as reduction in LA volume were found in 15 FD patients following ERT (median follow up 355 days) [66]. LA dilatation in FD may be due to higher LV filling pressures as a result of sphingolipid deposition, impaired diastolic relaxation and LVH but may also be due to direct sphingolipid deposition within the LA itself. Reduced peak LA reservoir function was confirmed in a further study of 22 FD adults on speckle-tracking echocardiography. These findings were notable because LA dilatation and impaired LA function correlated with the quantity of white matter lesions on cerebral MRI and high Fazekas score. The exact aetiology of white matter lesions in FD is uncertain but these data raise the possibility that altered atrial size and function may predispose the FD patient to atrial arrhythmia and stroke, in addition to simultaneous sphingolipid accumulation in the heart and brain [67].

6.4. Valve Disease

TTE is an essential imaging modality for the assessment and grading of valvular heart disease (VHD) associated with FD. A number of underlying mechanisms have been described as contributory factors predisposing to VHD in FD. In a retrospective study, in a cohort of 111 patients with FD, mild aortic, mitral, and tricuspid regurgitation was observed in patients with advanced Fabry cardiomyopathy [68]. Stenosis is uncommon in FD, and it has been hypothesized that direct sphingolipid accumulation in the fibrosa and laminose affects the structural integrity of the aortic valve in such a way as to compromise leaflet closure and promotes regurgitation. With mitral valve disease, a similar mechanism has been suggested but with the additional impact of altered annular motion, chordal retraction and papillary muscle hypertrophy secondary to myocardial changes in the LV (hypertrophy [69], fibrosis [37], and impairment [24]) (see Figure 10). In a similar way, atrial dilatation may alter chamber geometry and lead to functional mitral regurgitation and root dilatation seen in FD may contribute to aortic valve regurgitation [70]. In a recent retrospective cohort study, 100 adults with FD were assessed for valvular disease-burden, finding that VHD is common (10% had moderate to severe disease in at least one valve) and was associated with worsening renal function [71]. This compared with the estimated prevalence in of moderate or greater VHD in the general population of 5.2–6%. The high

prevalence observed in this recently published work is in contrast to previous cohort studies [68].
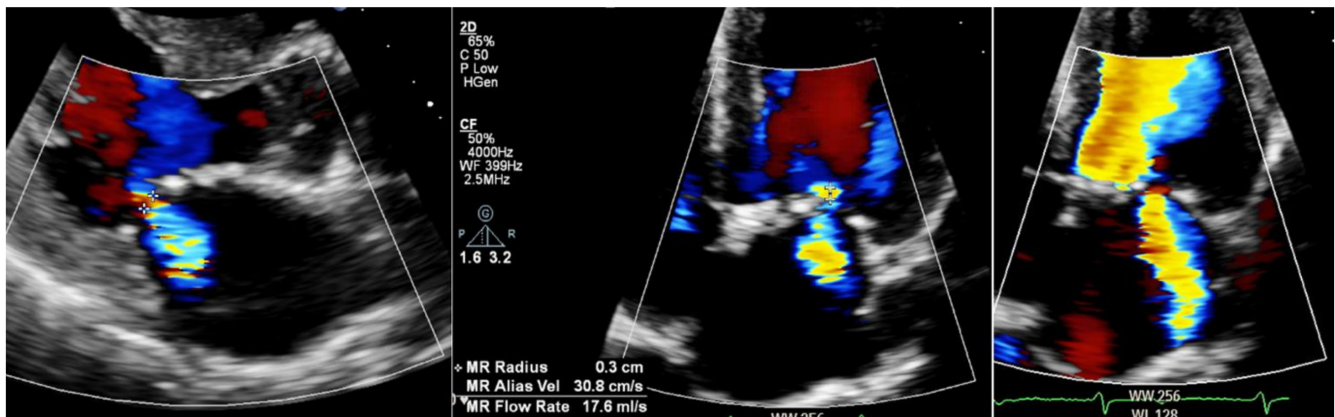

Figure 10. The 2D TTE MR assessment in an adult with advanced Fabry cardiomyopathy and co-existing end stage renal disease. (**Left**) Parasternal long axis view demonstrating LVH, left atrial dilatation, bilateral annular calcification of the mitral valve (causing basal restriction) with moderate MR evident on colour Doppler and vena contracta of 0.4 cm (moderate); (**Middle**) Apical 4-chamber view demonstrating bilateral annular calcification of the mitral valve with MR on colour Doppler and proximal isovelocity surface area (PISA) measurement of 0.3 cm (moderate); (**Right**) Apical 4-chamber view demonstrating moderate MR on colour Doppler.

7. Future Imaging

Cardiovascular imaging does not stand still, and there are many future developments that have huge potential in improving diagnosis, characterizing disease progression and selecting patients for appropriate treatment. T1 mapping has been an advance in early disease identification but is not all encompassing with a proportion of patients with normal T1 having other features that are subtle to suggest myocardial involvement. Finding a reliable method of characterizing these patients, or improving selection of patients for therapy, will require large scale studies with long-term follow-up. Future imaging modalities that may be relevant include shear wave elastography on high frame rate echocardiography or diffusion tensor imaging on CMR.

Shear wave elastography (SWE) has been used to assess stiffness within a tissue by measurement of propagation velocity of externally induced shear waves [72]. Shear-like waves have also been shown to naturally occur within myocardial tissue as a result of the impulse formed from closure of the mitral and aortic valve [73]. These can be measured using high rate TDI [74]. In a prospective study comparing normal volunteers with patients with HCM, shear wave velocities were measured using high frame rate TDI on TTE. The study demonstrated significantly higher shear wave velocities in the myocardium of HCM patients compared with normal volunteers which correlated with the E/e' ratio.

A clinical trial is currently underway to investigate the beneficial role of myocardial elastography as an assessment of myocardial stiffness in patients with FD and cardiac amyloidosis using a multifrequency convex transducer under specific adjustment to perform myocardial elastography [75]. SWE may provide a method of assessing for early diastolic changes in FD that could indicate early cardiomyopathy influencing decisions regarding commencement of disease-modifying treatment at an earlier stage.

Diffusion tensor CMR (DT-CMR) is an emerging tool providing a non-invasive assessment of microstructural cardiomyocyte organisation by assessing diffusion of water [76]. DT-CMR measures the effect of the cardiac microstructure on diffusion of water to gain information about myocardial organisation. Histological characteristics of HCM include cardiomyocyte disarray. DT-CMR provides a non-invasive technique of differentiating HCM phenotypes [77]. Within DT-CMR, measurement of apparent diffusion coefficient and the fractional anisotropy allow for quantification of disarray [78]. DT-CMR may provide

assessment of myocardial organisation and degree of disarray particularly in the early stages of sphingolipid accumulation in FD.

The use of AI in the detection of HCM using a 12-lead ECG has been demonstrated using AI-based convolutional neural networks (CNN) distinguishing HCM from non-HCM cases with low false-positive rates and good negative predictive value [79]. Future work could involve using CNN in the initial identification of FD using ECG criteria alongside automated echocardiography interpretation.

8. Conclusions

Advances in cardiac imaging techniques have enhanced our understanding of FD, such that it is now clear that sphingolipid accumulation within the heart is a continuous insidious process that precedes the development of LVH and can be identified early using advanced cardiac imaging, as described in this review. The identification of such findings may trigger clinicians to initiate treatment at an earlier stage where it is likely to have a more beneficial effect as opposed to when patients develop established cardiomyopathy where treatment is unlikely to be as efficacious. LA strain assessment, SWE and DT-CMR represent novel and emerging advances in the field of cardiac imaging that may support current techniques used within TTE and CMR to provide evidence of early cardiac involvement in FD, aiding both diagnostics and prognostication. These would further support the notion of commencing treatment at an earlier stage to reduce the burden cardiac mortality in FD.

References

1. Desnick, R.J.; Brady, R.; Barranger, J.; Collins, A.J.; Germain, D.P.; Goldman, M. Fabry disease, an under-recognized multisystemic disorder: Expert recommendations for diagnosis, management, and enzyme replacement therapy. *Ann. Intern Med.* **2003**, *138*, 338–346. [CrossRef]
2. Sweeley, C.C.; Klionsky, B. Fabry's disease: Classification as a sphingolipidosis and partial characterization of a novel glycolipid. *J. Biol. Chem.* **1963**, *238*, 3148–3150. [CrossRef]
3. Mehta, A.; Beck, M.; Eyskens, F.; Feliciani, C.; Kantola, I.; Ramaswami, U. Fabry disease: A review of current management strategies. *QJM Int. J. Med.* **2010**, *103*, 641–659. [CrossRef]
4. Linhart, A.; Germain, D.P.; Olivotto, I.; Akhtar, M.M.; Anastasakis, A.; Hughes, D. An expert consensus document on the management of cardiovascular manifestations of Fabry disease. *Eur. J. Heart Fail.* **2020**, *22*, 1076–1096. [CrossRef]
5. Hiwot, T.; Hughes, D.; Ramaswami, U. Guidelines for the treatment of Fabry Disease. *Br. Inherit. Metab. Dis. Group* **2020**, *2*, 1–10.
6. Yeung, D.F.; Sirrs, S.; Tsang, M.Y.; Gin, K.; Luong, C.; Jue, J.; Nair, P.; Lee, P.K.; Tsang, T.S. Echocardiographic Assessment of Patients with Fabry Disease. *J. Am. Soc. Echocardiogr.* **2018**, *31*, 639–649. [CrossRef]
7. Lang, R.M.; Badano, L.P.; Mor-Avi, V.; Afilalo, J.; Armstrong, A.; Ernande, L. Recommendations for cardiac chamber quantification by echocardiography in adults: An update from the American Society of Echocardiography and the European Association of Cardiovascular Imaging. *Eur. Heart J. Cardiovasc. Imaging* **2015**, *16*, 233–270. [CrossRef] [PubMed]
8. Captur, G.; Manisty, C.H.; Raman, B.; Marchi, A.; Wong, T.C.; Ariga, R. Maximal Wall Thickness Measurement in Hypertrophic Cardiomyopathy: Biomarker Variability and its Impact on Clinical Care. *JACC Cardiovasc. Imaging.* **2021**, *14*, 2123–2134. [CrossRef]

9.   Park, S.H.; Shub, C.; Nobrega, T.P.; Bailey, K.R.; Seward, J.B. Two-dimensional echocardiographic calculation of left ventricular mass as recommended by the American Society of Echocardiography: Correlation with autopsy and M-mode echocardiography. *J. Am. Soc. Echocardiogr.* **1996**, *9*, 119–128. [CrossRef]

10. Mor-Avi, V.; Sugeng, L.; Weinert, L.; MacEneaney, P.; Caiani, E.G.; Koch, R. Fast measurement of left ventricular mass with real-time three-dimensional echocardiography: Comparison with magnetic resonance imaging. *Circulation* **2004**, *110*, 1814–1818. [CrossRef]

11. Volpato, V.; Mor-Avi, V.; Narang, A.; Prater, D.; Gonçalves, A.; Tamborini, G.; Fusini, L.; Pepi, M.; Patel, A.R.; Lang, R.M. Automated, machine learning-based, 3D echocardiographic quantification of left ventricular mass. *Echocardiography* **2019**, *36*, 312–319. [CrossRef]

12. O'Brien, C.; Britton, I.; Karur, G.R.; Iwanochko, R.M.; Morel, C.F.; Nguyen, E.T. Left Ventricular Mass and Wall Thickness Measurements Using Echocardiography and Cardiac MRI in Patients with Fabry Disease: Clinical Significance of Discrepant Findings. *Radiol. Cardiothorac. Imaging* **2020**, *2*, e190149. [CrossRef] [PubMed]

13. Hazari, H.; Belenkie, I.; Kryski, A.; White, J.A.; Oudit, G.Y.; Thompson, R. Comparison of Cardiac Magnetic Resonance Imaging and Echocardiography in Assessment of Left Ventricular Hypertrophy in Fabry Disease. *Can. J. Cardiol.* **2018**, *34*, 1041–1047. [CrossRef] [PubMed]

14. Maceira, A.M.; Prasad, S.K.; Khan, M.; Pennell, D. Normalized left ventricular systolic and diastolic function by steady state free precession cardiovascular magnetic resonance. *J. Cardiovasc. Magn. Reson.* **2006**, *8*, 417–426. [CrossRef]

15. Petersen, S.E.; Aung, N.; Sanghvi, M.; Zemrak, F.; Fung, K.; Paiva, J.M.; Francis, J.M.; Khanji, M.Y.; Lukaschuk, E.; Lee, A.; et al. Reference ranges for cardiac structure and function using cardiovascular magnetic resonance (CMR) in Caucasians from the UK Biobank population cohort. *J. Cardiovasc. Magn. Reson.* **2017**, *19*, 18. [CrossRef]

16. Moody, W.E.; Hudsmith, L.E.; Holloway, B.; Treibel, T.A.; Davies, R.; Kozor, R. Variation in cardiovascular magnetic resonance myocardial contouring: Insights from an international survey. *J. Magn. Reson. Imaging* **2019**, *50*, 1336–1338. [CrossRef]

17. Augusto, J.B.; Davies, R.H.; Bhuva, A.N.; Knott, K.D.; Seraphim, A.; Alfarih, M. Diagnosis and risk stratification in hypertrophic cardiomyopathy using machine learning wall thickness measurement: A comparison with human test-retest performance. *Lancet Digit. Health* **2021**, *3*, e20–e28. [CrossRef]

18. Arends, M.; Wanner, C.; Hughes, D.; Mehta, A.; Oder, D.; Watkinson, O.T.; Elliott, P.M.; Linthorst, G.E.; Wijburg, F.A.; Biegstraaten, M.; et al. Characterization of Classical and Nonclassical Fabry Disease: A Multicenter Study. *J. Am. Soc. Nephrol.* **2017**, *28*, 1631–1641. [CrossRef]

19. Vijapurapu, R.; Baig, S.; Nordin, S.; Augusto, J.; Price, A.M.; Wheeldon, N.; Lewis, N.; Kozor, R.; Kotecha, D.; Hodson, J.; et al. Longitudinal Assessment of Cardiac Involvement in Fabry Disease Using Cardiovascular Magnetic Resonance Imaging. *JACC Cardiovasc. Imaging* **2020**, *13*, 1850–1852. [CrossRef]

20. Nordin, S.; Kozor, R.; Vijapurapu, R.; Augusto, J.; Knott, K.D.; Captur, G.; Treibel, T.; Ramaswami, U.; Tchan, M.; Geberhiwot, T.; et al. Myocardial Storage, Inflammation, and Cardiac Phenotype in Fabry Disease After One Year of Enzyme Replacement Therapy. *Circ. Cardiovasc. Imaging* **2019**, *12*, e009430. [CrossRef]

21. Ho, C.; Sweitzer, N.K.; McDonough, B.; Maron, B.J.; Casey, S.A.; Seidman, J.; Seidman, C.E.; Solomon, S.D. Assessment of diastolic function with Doppler tissue imaging to predict genotype in preclinical hypertrophic cardiomyopathy. *Circulation* **2002**, *105*, 2992–2997. [CrossRef]

22. Pieroni, M.; Chimenti, C.; Ricci, R.; Sale, P.; Russo, M.A.; Frustaci, A. Early detection of Fabry cardiomyopathy by tissue Doppler imaging. *Circulation* **2003**, *107*, 1978–1984. [CrossRef] [PubMed]

23. Zamorano, J.; Serra, V.; de Isla, L.P.; Feltes, G.; Calli, A.; Barbado, F.J.; Torras, J.; Hernandez, S.; Herrera, J.; Herrero, J.A.; et al. Usefulness of tissue Doppler on early detection of cardiac disease in Fabry patients and potential role of enzyme replacement therapy (ERT) for avoiding progression of disease. *Eur. J. Echocardiogr.* **2011**, *12*, 671–677. [CrossRef] [PubMed]

24. Weidemann, F.; Breunig, F.; Beer, M.; Knoll, A.; Turschner, O.; Wanner, C.; Sandstede, J.; Voelker, W.; Ertl, G.; Strotmann, J. Improvement of cardiac function during enzyme replacement therapy in patients with Fabry disease: A prospective strain rate imaging study. *Circulation* **2003**, *108*, 1299–1301. [CrossRef]

25. Weidemann, F.; Niemann, M.; Breunig, F.; Herrmann, S.; Beer, M.; Störk, S. Long-term effects of enzyme replacement therapy on fabry cardiomyopathy: Evidence for a better outcome with early treatment. *Circulation* **2009**, *119*, 524–529. [CrossRef]

26. Shanks, M.; Thompson, R.; Paterson, D.I.; Putko, B.; Khan, A.; Chan, A.; Becher, H.; Oudit, G.Y. Systolic and diastolic function assessment in fabry disease patients using speckle-tracking imaging and comparison with conventional echocardiographic measurements. *J. Am. Soc. Echocardiogr.* **2013**, *26*, 1407–1414. [CrossRef]

27. Faggiano, A.; Avallone, C.; Gentile, D.; Provenzale, G.; Toriello, F.; Merlo, M.; Sinagra, G.; Carugo, S. Echocardiographic Advances in Di-lated Cariomyopathy. *J. Clin. Med.* **2021**, *10*, 5518. [CrossRef]

28. Sado, D.M.; White, S.K.; Piechnik, S.K.; Banypersad, S.M.; Treibel, T.; Captur, G. Identification and assessment of Anderson-Fabry disease by cardiovascular magnetic resonance noncontrast myocardial T1 mapping. *Circ. Cardiovasc. Imaging* **2013**, *6*, 392–398. [CrossRef] [PubMed]

29. Nordin, S.; Kozor, R.; Baig, S.; Abdel-Gadir, A.; Medina-Menacho, K.; Rosmini, S.; Captur, G.; Tchan, M.; Geberhiwot, T.; Murphy, E.; et al. Cardiac Phenotype of Prehypertrophic Fabry Disease. *Circ. Cardiovasc. Imaging* **2018**, *11*, e007168. [CrossRef]

30. Pica, S.; Sado, D.M.; Maestrini, V.; Fontana, M.; White, S.K.; Treibel, T.; Captur, G.; Anderson, S.; Piechnik, S.K.; Robson, M.D.; et al. Reproducibility of native myocardial T1 mapping in the assessment of Fabry disease and its role in early detection of cardiac involvement by cardiovascular magnetic resonance. *J. Cardiovasc. Magn. Reson.* **2014**, *16*, 1–9. [CrossRef]

31. Camporeale, A.; Pieroni, M.; Pieruzzi, F.; Lusardi, P.; Pica, S.; Spada, M. Predictors of Clinical Evolution in Prehypertrophic Fabry Disease. *Circ. Cardiovasc. Imaging* **2019**, *12*, e008424. [CrossRef] [PubMed]

32. Knott, K.D.; Augusto, J.B.; Nordin, S.; Kozor, R.; Camaioni, C.; Xue, H.; Hughes, R.K.; Manisty, C.; Brown, L.A.E.; Kellman, P.; et al. Quantitative Myocardial Perfusion in Fabry Disease. *Circ. Cardiovasc. Imaging* **2019**, *12*, e008872. [CrossRef] [PubMed]

33. Dass, S.; Suttie, J.J.; Piechnik, S.K.; Ferreira, V.M.; Holloway, C.J.; Banerjee, R.; Mahmod, M.; Cochlin, L.; Karamitsos, T.D.; Robson, M.D.; et al. Myocardial tissue characterization using magnetic resonance noncontract t1 mapping in hypertrophic and dilated cardiomyopathy. *Circ. Cardiovasc. Imaging* **2012**, *5*, 726–733. [CrossRef] [PubMed]

34. Seydelmann, N.; Liu, D.; Krämer, J.; Drechsler, C.; Hu, K.; Nordbeck, P. High-Sensitivity Troponin: A Clinical Blood Biomarker for Staging Cardiomyopathy in Fabry Disease. *J. Am. Heart Assoc.* **2016**, *5*, e002839. [CrossRef] [PubMed]

35. Hughes, D.A.; Aguiar, P.; Deegan, P.B.; Ezgu, F.; Frustaci, A.; Lidove, O. Early indicators of disease progression in Fabry disease that may indicate the need for disease-specific treatment initiation: Findings from the opinion-based PREDICT-FD modified Delphi consensus initiative. *BMJ Open* **2020**, *10*, e035182. [CrossRef]

36. Nordin, S.; Kozor, R.; Menacho, K.; Abdel-Gadir, A.; Baig, S.; Sado, D.M.; Lobascio, I.; Murphy, E.; Lachmann, R.H.; Mehta, A.; et al. Proposed Stages of Myocardial Phenotype Development in Fabry Disease. *JACC Cardiovasc. Imaging.* **2019**, *12*, 1673–1683. [CrossRef]

37. Moon, J.; Sachdev, B.; Elkington, A.G.; McKenna, W.J.; Mehta, A.; Pennell, D.; Leed, P.J.; Elliott, P. Gadolinium enhanced cardiovascular magnetic resonance in Anderson-Fabry disease. Evidence for a disease specific abnormality of the myocardial interstitium. *Eur. Heart J.* **2003**, *24*, 2151–2155. [CrossRef]

38. Augusto, J.; Nordin, S.; Vijapurapu, R.; Baig, S.; Bulluck, H.; Castelletti, S.; Alfarih, M.; Knott, K.; Captur, G.; Kotecha, T.; et al. Myocardial Edema, Myocyte Injury, and Disease Severity in Fabry Disease. *Circ. Cardiovasc. Imaging* **2020**, *13*, e010171. [CrossRef]

39. Imbriaco, M.; Nappi, C.; Ponsiglione, A.; Pisani, A.; Dell'Aversana, S.; Nicolai, E. Hybrid positron emission tomography-magnetic resonance imaging for assessing different stages of cardiac impairment in patients with Anderson-Fabry disease: AFFINITY study group. *Eur. Heart J. Cardiovasc. Imaging* **2019**, *20*, 1004–1011. [CrossRef]

40. Spinelli, L.; Imbriaco, M.; Nappi, C.; Nicolai, E.; Giugliano, G.; Ponsiglione, A. Early Cardiac Involvement Affects Left Ventricular Longitudinal Function in Females Carrying α-Galactosidase A Mutation: Role of Hybrid Positron Emission Tomography and Magnetic Resonance Imaging and Speckle-Tracking Echocardiography. *Circ. Cardiovasc. Imaging* **2018**, *11*, e007019. [CrossRef] [PubMed]

41. Yogasundaram, H.; Nikhanj, A.; Putko, B.N.; Boutin, M.; Jain-Ghai, S.; Khan, A.; Auray-Blais, C.; West, M.L.; Oudit, G.Y. Elevated Inflammatory Plasma Biomarkers in Patients with Fabry Disease: A Critical Link to Heart Failure with Preserved Ejection Fraction. *J. Am. Heart Assoc.* **2018**, *7*, e009098. [CrossRef]

42. Patel, M.R.; Cecchi, F.; Cizmarik, M.; Kantola, I.; Linhart, A.; Nicholls, K.; Strotmann, J.; Tallaj, J.; Tran, T.C.; West, M.L.; et al. Cardiovascular events in patients with fabry disease natural history data from the fabry registry. *J. Am. Coll. Cardiol.* **2011**, *57*, 1093–1099. [CrossRef]

43. Feriozzi, S.; Linhart, A.; Ramaswami, U.; Kalampoki, V.; Gurevich, A.; Hughes, D. Effects of Baseline Left Ventricular Hypertrophy and Decreased Renal Function on Cardiovascular and Renal Outcomes in Patients with Fabry Disease Treated with Agalsidase Alfa: A Fabry Outcome Survey Study. *Clin. Ther.* **2020**, *42*, 2321–2330. [CrossRef] [PubMed]

44. Spinelli, L.; Giugliano, G.; Pisani, A.; Imbriaco, M.; Imbriaco, M.; Riccio, E.; Russo, C.; Cuocolo, A.; Trimarco, B.; Esposito, G. Does left ven-tricular function predict cardiac outcome in Anderson-Fabry disease. *Int. J. Cardiovasc. Imaging* **2021**, *27*, 1225–1236. [CrossRef]

45. Hopkin, R.J.; Cabrera, G.; Charrow, J.; Lemay, R.; Martins, A.M.; Mauer, M.; Ortiz, A.; Patel, M.R.; Sims, K.; Waldek, S.; et al. Risk factors for severe clinical events in male and female patients with Fabry disease treated with agalsidase beta enzyme replacement therapy: Data from the Fabry Registry. *Mol. Genet. Metab.* **2016**, *119*, 151–159. [CrossRef] [PubMed]

46. Krämer, J.; Niemann, M.; Störk, S.; Frantz, S.; Beer, M.; Ertl, G. Relation of burden of myocardial fibrosis to malignant ventricular arrhythmias and outcomes in Fabry disease. *Am. J. Cardiol.* **2014**, *114*, 895–900. [CrossRef] [PubMed]

47. Zegard, A.; Okafor, O.; de Bono, J.; Kalla, M.; Lencioni, M.; Marshall, H.; Hudsmith, L.; Qiu, T.; Steeds, R.; Stegemann, B.; et al. Myocardial Fibrosis as a Predictor of Sudden Death in Patients with Coronary Artery Disease. *J. Am. Coll. Cardiol.* **2021**, *77*, 29–41. [CrossRef]

48. Di Marco, A.; Anguera, I.; Schmitt, M.; Klem, I.; Neilan, T.G.; White, J.A. Late Gadolinium Enhancement and the Risk for Ventricular Arrhythmias or Sudden Death in Dilated Cardiomyopathy: Systematic Review and Meta-Analysis. *JACC Heart Fail.* **2017**, *5*, 28–38. [CrossRef]

49. Tomberli, B.; Cecchi, F.; Sciagrà, R.; Berti, V.; Lisi, F.; Torricelli, F.; Morrone, A.; Castelli, G.; Yacoub, M.H.; Olivotto, I. Coronary microvascular dysfunction is an early feature of cardiac involvement in patients with Anderson-Fabry disease. *Eur. J. Heart Fail.* **2013**, *15*, 1363–1373. [CrossRef]

50. Spinelli, L.; Imbriaco, M.; Giugliano, G.; Nappi, C.; Gaudieri, V.; Riccio, E.; Pisani, A.; Trimarco, B.; Cuocolo, A. Focal reduction in left ventricular. *J. Nucl. Cardiol.* **2021**, *28*, 641–649. [CrossRef]

51. Chimenti, C.; Morgante, E.; Tanzilli, G.; Mangieri, E.; Critelli, G.; Gaudio, C.; Russo, M.A.; Frustaci, A. Angina in fabry disease reflects coronary small vessel disease. *Circ. Heart Fail.* **2008**, *1*, 161–169. [CrossRef] [PubMed]
52. Roy, A.; Umar, H.; Ochoa-Ferraro, A.; Warfield, A.; Lewis, N.; Geberhiwot, T. Atherosclerosis in Fabry Disease—A Contemporary Review. *J. Clin. Med.* **2021**, *10*, 4422. [CrossRef] [PubMed]
53. Brown, L.K.; Miller, A.; Bhuptani, A.; Sloane, M.F.; I Zimmerman, M.; Schilero, G.; Eng, C.M.; Desnick, R.J. Pulmonary involvement in Fabry disease. *Am. J. Respir. Crit. Care Med.* **1997**, *155*, 1004–1010. [CrossRef]
54. Franzen, D.; Krayenbuehl, P.A.; Lidove, O.; Aubert, J.D.; Barbey, F. Pulmonary involvement in Fabry disease: Overview and perspectives. *Eur. J. Intern. Med.* **2013**, *24*, 707–713. [CrossRef] [PubMed]
55. Wang, R.Y.; Abe, J.T.; Cohen, A.H.; Wilcox, W.R. Enzyme replacement therapy stabilizes obstructive pulmonary Fabry disease associated with respiratory globotriaosylceramide storage. *J. Inherit. Metab. Dis.* **2008**, *31* (Suppl. S2), S369–S374. [CrossRef]
56. Wang, R.Y.; Lelis, A.; Mirocha, J.; Wilcox, W.R. Heterozygous Fabry women are not just carriers, but have a significant burden of disease and impaired quality of life. *Genet. Med.* **2007**, *9*, 34–45. [CrossRef]
57. Koskenvuo, J.W.; Kantola, I.M.; Nuutila, P.; Knuuti, J.; Parkkola, R.; Mononen, I.; Hurme, S.; Kalliokoski, R.; Viikari, J.S.; Wendelin-Saarenhovi, M.; et al. Cardiopulmonary involvement in Fabry's disease. *Acta Cardiol.* **2010**, *65*, 185–192. [CrossRef]
58. Vilcant, V.; Hai, O. *Left Ventricular Outflow Tract Obstruction*; StatPearls: Treasure Island, FL, USA, 2021.
59. Wu, J.C.; Ho, C.Y.; Skali, H.; Abichandani, R.; Wilcox, W.R.; Banikazemi, M.; Packman, S.; Sims, K.; Solomon, S.D. Cardiovascular manifestations of Fabry disease: Relationships between left ventricular hypertrophy, disease severity, and alpha-galactosidase A activity. *Eur. Heart J.* **2010**, *31*, 1088–1097. [CrossRef]
60. Calcagnino, M.; O'Mahony, C.; Coats, C.; Cardona, M.; Garcia, A.; Janagarajan, K.; Mehta, A.; Hughes, D.; Murphy, E.; Lachmann, R.; et al. Exercise-induced left ventricular outflow tract obstruction in symptomatic patients with Anderson-Fabry disease. *J. Am. Coll. Cardiol.* **2011**, *58*, 88–89. [CrossRef]
61. Baig, S.; Edward, N.C.; Kotecha, D.; Liu, B.; Nordin, S.; Kozor, R.; Moon, J.C.; Geberhiwot, T.; Steeds, R.P. Ventricular arrhythmia and sudden cardiac death in Fabry disease: A systematic review of risk factors in clinical practice. *Europace* **2018**, *20*, F153–F161. [CrossRef]
62. Issac, T.T.; Dokainish, H.; Lakkis, N.M. Role of inflammation in initiation and perpetuation of atrial fibrillation: A systematic review of the published data. *J. Am. Coll. Cardiol.* **2007**, *50*, 2021–2028. [CrossRef] [PubMed]
63. Seko, Y.; Kato, T.; Haruna, T.; Izumi, T.; Miyamoto, S.; Nakane, E.; Inoko, M. Association between atrial fibrillation, atrial enlargement, and left ventricular geometric remodeling. *Sci. Rep.* **2018**, *8*, 6366. [CrossRef] [PubMed]
64. Donal, E.; Lip, G.Y.H.; Galderisi, M.; Goette, A.; Shah, D.; Marwan, M.; Lederlin, M.; Mondillo, S.; Edvardsen, T.; Sitges, M.; et al. EACVI/EHRA Expert Consensus Document on the role of multi-modality imaging for the evaluation of patients with atrial fibrillation. *Eur. Heart J. Cardiovasc. Imaging* **2016**, *17*, 355–383. [CrossRef] [PubMed]
65. Boyd, A.C.; Lo, Q.; Devine, K.; Tchan, M.C.; Sillence, D.O.; Sadick, N.; Richards, D.A.; Thomas, L. Left atrial enlargement and reduced atrial compliance occurs early in Fabry cardiomyopathy. *J. Am. Soc. Echocardiogr.* **2013**, *26*, 1415–1423. [CrossRef] [PubMed]
66. Pichette, M.; Serri, K.; Pagé, M.; Di, L.Z.; Bichet, D.G.; Poulin, F. Impaired Left Atrial Function in Fabry Disease: A Longitudinal Speckle-Tracking Echocardiography Study. *J. Am. Soc. Echocardiogr.* **2017**, *30*, 170–179.e2. [CrossRef] [PubMed]
67. Esposito, R.; Russo, C.; Santoro, C.; Cocozza, S.; Riccio, E.; Sorrentino, R.; Pontillo, G.; Luciano, F.; Imbriaco, M.; Brunetti, A.; et al. Association between Left Atrial Deformation and Brain Involvement in Patients with Anderson-Fabry Disease at Diagnosis. *J. Clin. Med.* **2020**, *9*, 2741. [CrossRef]
68. Weidemann, F.; Strotmann, J.M.; Niemann, M.; Herrmann, S.; Wilke, M.; Beer, M. Heart valve involvement in Fabry cardiomyopathy. *Ultrasound Med. Biol.* **2009**, *35*, 730–735. [CrossRef]
69. Linhart, A.; Kampmann, C.; Zamorano, J.L.; Sunder-Plassmann, G.; Beck, M.; Mehta, A. Cardiac manifestations of Anderson-Fabry disease: Results from the international Fabry outcome survey. *Eur. Heart J.* **2007**, *28*, 1228–1235. [CrossRef]
70. Barbey, F.; Qanadli, S.D.; Juli, C.; Brakch, N.; Palaček, T.; Rizzo, E.; Jeanrenaud, X.; Eckhardt, B.; Linhart, A. Aortic remodelling in Fabry disease. *Eur. Heart J.* **2010**, *31*, 347–353. [CrossRef]
71. Yogasundaram, H.; Nikhanj, A.; Chatur, S.; Qi, A.; Hagen, L.; Bailey, L.; Khan, A.; Hopkin, R.J.; Fine, N.M.; Jefferies, J.L.; et al. Burden of Valvular Heart Disease in Patients with Fabry Disease. *J. Am. Soc. Echocardiogr.* **2021**, *21*, 762–768. [CrossRef]
72. Shiina, T.; Nightingale, K.R.; Palmeri, M.L.; Hall, T.J.; Bamber, J.C.; Barr, R.G.; Castera, L.; Choi, B.I.; Chou, Y.-H.; Cosgrove, D.; et al. WFUMB guidelines and recommendations for clinical use of ultrasound elastography: Part 1: Basic principles and terminology. *Ultrasound Med. Biol.* **2015**, *41*, 1126–1147. [CrossRef]
73. Brekke, B.; Nilsen, L.C.; Lund, J.; Torp, H.; Bjastad, T.; Amundsen, B.H.; Stoylen, A.; Aase, S.A. Ultra-high frame rate tissue Doppler imaging. *Ultrasound Med. Biol.* **2014**, *40*, 222–231. [CrossRef]
74. Strachinaru, M.; Bosch, J.G.; van Dalen, B.M.; van Gils, L.; van der Steen, A.F.W.; de Jong, N. Cardiac Shear Wave Elastography Using a Clinical Ultrasound System. *Ultrasound Med. Biol.* **2017**, *43*, 1596–1606. [CrossRef] [PubMed]
75. Fernandes, F.; Cafezeiro, C. *NCT04456582 Noninvasive Assessment of Myocardial Stiffness by 2D-SWE Ultrasound Technique (Two-Dimensional Shear Wave Elastography) in Patients with Amyloidosis and Fabry Disease (FABRY)*; U.S. National Library of Medicine: Bethesda, MD, USA, 2021.
76. Khalique, Z.; Ferreira, P.F.; Scott, A.D.; Nielles-Vallespin, S.; Firmin, D.N.; Pennell, D.J. Diffusion Tensor Cardiovascular Magnetic Resonance Imaging: A Clinical Perspective. *JACC Cardiovasc. Imaging* **2020**, *13*, 1235–1255. [CrossRef]

77.   Lewis, A.J.M.; Rider, O.J. The use of cardiovascular magnetic resonance for the assessment of left ventricular hypertrophy. *Cardiovasc. Diagn. Ther.* **2020**, *10*, 568–582. [CrossRef] [PubMed]

78.   Caredda, G.; Bassareo, P.P.; Cherchi, M.V.; Pontone, G.; Suri, J.S.; Saba, L. Anderson-fabry disease: Role of traditional and new cardiac MRI techniques. *Br. J. Radiol.* **2021**, *94*, 20210020. [CrossRef] [PubMed]

79.   Ko, W.-Y.; Siontis, K.C.; Attia, Z.I.; Carter, R.E.; Kapa, S.; Ommen, S.R.; Demuth, S.J.; Ackerman, M.J.; Gersh, B.J.; Arruda-Olson, A.M.; et al. Detection of Hypertrophic Cardiomyopathy Using a Convolutional Neural Network-Enabled Electrocardiogram. *J. Am. Coll. Cardiol.* **2020**, *75*, 722–733. [CrossRef] [PubMed]